

Polynomial Solution to the Position Analysis of Two Assur Kinematic Chains With Four Loops and the Same Topology

Júlia Borràs

Institut de Robòtica i Informàtica Industrial
(UPC-CSIC),
Barcelona 08028, Spain
e-mail: jborras@iri.upc.edu

Raffaele Di Gregorio¹

Department of Engineering (EnDiF),
University of Ferrara,
Ferrara 44100, Italy
e-mail: rdigregorio@ing.unife.it

The direct position analysis (DPA) of a manipulator is the computation of the end-effector poses (positions and orientations) compatible with assigned values of the actuated-joint variables. Assigning the actuated-joint variables corresponds to considering the actuated joints locked, which makes the manipulator a structure. The solutions of the DPA of a manipulator one to one correspond to the assembly modes of the structure that is generated by locking the actuated-joint variables of that manipulator. Determining the assembly modes of a structure means solving the DPA of a large family of manipulators since the same structure can be generated from different manipulators. This paper provides an algorithm that determines all the assembly modes of two structures with the same topology that are generated from two families of mechanisms: one planar and the other spherical. The topology of these structures is constituted of nine links (one quaternary link, four ternary links, and four binary links) connected through 12 revolute pairs to form four closed loops. [DOI: 10.1115/1.3046134]

Keywords: parallel mechanisms, kinematics, position analysis, Assur kinematic chains

1 Introduction

The direct position analysis (DPA) of a manipulator is the computation of the end-effector poses (positions and orientations) compatible with assigned values of the actuated-joint variables. Assigning the actuated-joint variables corresponds to considering the actuated joints locked, which makes the manipulator a structure. The solutions of the DPA of a manipulator one to one correspond to the assembly modes of the structure generated by locking the actuated-joint variables of that manipulator. Determining the assembly modes of a structure means solving the DPA of a large family of manipulators since the same structure can be generated from different manipulators.

The solution of the DPA of parallel manipulators (PMs) is a difficult and challenging task since, in general, it involves the solution of a system of nonlinear equations.

Spherical parallel manipulators (SPMs) are PMs where the end-effector performs only spherical motions with a center fixed to the frame. SPMs can be collected into two subsets: (i) the set of the SPMs where only the end-effector and few (or no) other links perform spherical motions with the same center and (ii) the set of the SPMs where all the links perform spherical motions with the same center. When the actuated joints are locked, both these two types of SPMs become structures whose assembly modes can be identified by considering equivalent structures where the links are connected only through revolute pairs with axes that converge toward the spherical motion center. Such structures will be called spherical structures (SSs).

Structures composed of links connected only through revolute pairs are also generated from a large family of planar parallel manipulators (PPMs) by locking the actuated joints. In this case,

all the revolute-pair axes are parallel to one another and perpendicular to the plane of motion. Such structures will be called planar structures (PSs).

When the topology of a structure is analyzed, only the number and the type (binary, ternary, etc.) of links and the type of kinematic pairs that connect the links to one another are considered. Therefore, the SSs and the PSs share the same set of topologies.

Moreover, by using the Grübler–Kutzbach equation, it is easy to demonstrate that, in the SSs and the PSs, the number of loops, l , the number of links, m , and the number of revolute pairs, r , are related by the following two relationships: $m=2l+1$ and $r=3l$.

Sometimes structures contain substructures (i.e., a subset of links that form a structure by themselves). A substructure can be substituted into the original structure by a unique link whose shape depends on the assembly modes of the substructure. This substitution process ends when no other substructure can be identified in the last obtained structure. In literature, structures that do not contain substructures have been called Assur kinematic chains (AKCs). The determination of all the assembly modes of any structure can be implemented by exploiting a set of algorithms that solve all the AKCs [1].

The solution of the DPA of all the SPMs can be implemented by classifying all the SS topologies, which refer to AKCs, and then by providing, for each identified topology, an algorithm that computes the assembly modes of the AKC with that topology. The fact that the set of SS topologies coincides with the one of PSs allows the wide literature on planar mechanisms to be exploited [2]. In particular (see Ref. [1]), there are one single-loop AKC topology (the triad), one double-loop AKC topology (the pentad), and three triple-loop AKC topologies. Moreover, Manolescu [3] gave a complete classification of triple-loop topologies and how they are built. Eventually, Yang and Yao [4] identified all the AKC topologies with four loops. So doing, they showed that there are 28 quadruple-loop AKC topologies (see also Refs. [5] and [9]).

The algorithms that analytically calculate all the assembly modes of the AKCs up to three loops have been already presented both for the planar case (see Ref. [1] for references) and for the spherical case (see Ref. [2] for references). Moreover, general

¹Corresponding author.

Contributed by the Mechanisms and Robotics Committee of ASME for publication in the JOURNAL OF MECHANISMS AND ROBOTICS. Manuscript received March 30, 2008; final manuscript received August 30, 2008; published online January 6, 2009. Review conducted by Qizheng Liao.

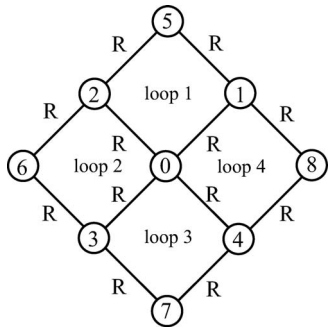


Fig. 1 Topology of the studied structures: graph vertices represent links and graph edges represent joints (*R* stands for revolute pair)

techniques for solving the DPA of planar mechanisms have been presented (see, for instance, Refs. [6–8]), and the assembly modes of a number of planar structures with four loops have been analytically determined (see Ref. [9] for references). As far as the authors are aware the determination of the assembly modes of spherical structures with four loops was not addressed yet.

This paper addresses the determination of the assembly modes of the structures, either planar or spherical, with 1 out of the 28 quadruple-loop AKC topologies (the 15th one reported in Table 1 of Ref. [9]). And it provides one algorithm, which is applicable to the planar and the spherical cases and solves the closure-equation systems of these structures in analytical form. In particular, the topology of these structures is the one reported in Fig. 1, and it is constituted of nine links (one quaternary link, four ternary links, and four binary links) connected through 12 revolute pairs to form four closed loops.

The planar structure with this topology has been already solved in Ref. [10] by using an algorithm based on complex numbers and similar to the ones reported in Refs. [9] and [11]. The solution technique used in Ref. [10] is different from the one reported here and cannot be extended to the spherical structure with the same topology.

2 Background

The closure equations of a structure (or a mechanism) can be written in many ways. The most common techniques are based on the use of the loop equations that are a fixed number, say, n , of independent scalar equations that can be written for each independent loop appearing in the structure.

When the structure contains a number of particular binary links at least equal to the number of independent loops, and the choice of the independent loops can be operated so that each loop contains at least one binary link not included in the other loops, the number n can be reduced to 1, and the closure-equation system can be reduced to a number of scalar equations equal to the number of loops.

The analysis of Fig. 1 reveals that, in the structures under study, four independent loops with one binary link can be easily individuated: (1) loop 0-1-5-2 (link 5 is binary), (2) loop 0-2-6-3 (link 6 is binary), (3) loop 0-3-7-4 (link 7 is binary), and (4) loop 0-4-8-1 (link 8 is binary). All these loops are four-bar loops with only revolute pairs.

Both in the planar case and in the spherical case, the revolute-pair axes are located by points lying on the motion plane² (planar case) or on the unit sphere³ (spherical case). In our case, this

²The motion plane is a plane surface perpendicular to all the revolute-pair axes.

³The unit sphere is a sphere surface with unit radius and center coincident with the center of the spherical motion. It is worth noting that the unit sphere is perpendicular to all the revolute-pair axes since all the revolute-pair axes converge toward the center of the spherical motion.

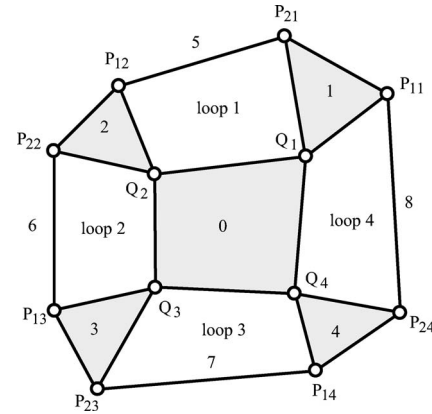


Fig. 2 Four-loop PS with the topology of Fig. 1

technique simply consists in writing, for each loop, that the distance (either on the motion plane or on the unit sphere⁴) between the two points locating the revolute-pair axes at the endings of the binary link is constant.

In Sec. 3 this technique will be used to write a minimal set of closure equations both for the planar case and for the spherical case.

3 Closure Equations

By using the above-mentioned technique to write the closure equations, the resulting closure equations are very similar in the two cases under study, and the same elimination technique can be adopted for determining a univariate polynomial equation to solve.

In Secs. 3.1 and 3.2, the closure-equation system will be deduced for both the cases.

3.1 Planar Structure. Figure 2 shows the planar structure with the topology of Fig. 1. With reference to Fig. 2, Q_i for $i=1, \dots, 4$ are the points that locate the axes of the revolute pairs that join the quaternary link (link 0) to the i th ternary link ($i=1, \dots, 4$). P_{ji} for $j=1, 2$ and $i=1, \dots, 4$ are the points that locate the axes of the revolute pairs that join the i th ternary link to the two adjacent binary links.

Figure 3 shows the i th loop ($i=1, \dots, 4$) of the PS and the notation that will be used to deduce its loop equation. With reference to Fig. 3, the link-index k is equal to $(i+1)$ modulo 4. r_{0i} is the length of the segment $Q_i Q_k$. r_{ji} (r_{jk}), $j=1, 2$, is the length of the segment $Q_i P_{ji}$ ($Q_k P_{jk}$). And $r_{3(i+4)}$ is the length of the segment $P_{2i} P_{1k}$. The angles β_i and γ_i (β_k and γ_k) are the interior angles at Q_i (Q_k) of link i (link k) and link 0, respectively. The angle θ_i (θ_k) is the joint variable of the revolute pair located by Q_i (Q_k). Eventually, the reference system $Q_i x_i y_i$ is a Cartesian reference system, fixed to link 0, that will be used to write the loop equation of the i th loop.

It is worth noting that the eight geometric constants of the quaternary link (i.e., γ_i and r_{0i} for $i=1, \dots, 4$) are related by the following three scalar equations (see Figs. 2 and 3):

$$\sum_{i=1}^4 \gamma_i = 2\pi \quad (1a)$$

$$r_{01} - r_{02} \cos \gamma_2 = r_{04} \cos \gamma_1 - r_{03} \cos(\gamma_1 + \gamma_4) \quad (1b)$$

⁴The distance between two points on a sphere surface is the length of the shortest great-circle arc joining the two points. On the unit sphere, this distance coincides with the convex central angle delimited by the two radii passing through the two points if the angle is measured in radians.

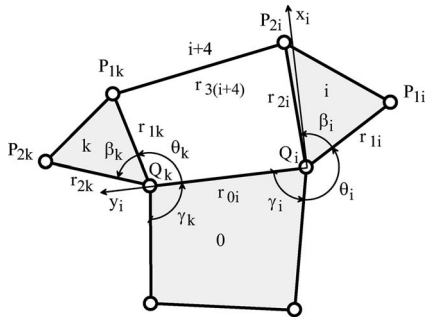


Fig. 3 i th loop of the PS: notation ($i=1, \dots, 4$; $k=(i+1)$ modulo 4)

$$r_{02} \sin \gamma_2 = r_{04} \sin \gamma_1 - r_{03} \sin(\gamma_1 + \gamma_4) \quad (1c)$$

With these notations, the position vectors of the points P_{2i} and P_{1k} , in the reference system $Q_i x_i y_i$, have the following explicit expressions ($i=1, \dots, 4$; $k=(i+1)$ modulo 4):

$${}^i \mathbf{P}_{2i} = \begin{pmatrix} a_i c_i - b_i s_i \\ a_i s_i + b_i c_i \end{pmatrix}, \quad {}^i \mathbf{P}_{1k} = \begin{pmatrix} r_{1k} s_k \\ r_{0i} - r_{1k} c_k \end{pmatrix} \quad (2)$$

where the left superscript i indicates that the vectors are measured in $Q_i x_i y_i$. c_i (c_k) and s_i (s_k) stand for $\cos \theta_i$ ($\cos \theta_k$) and $\sin \theta_i$ ($\sin \theta_k$), respectively. Eventually, a_i and b_i are geometric constants with the following explicit expressions:

$$a_i = r_{2i} \cos(\gamma_i + \beta_i - \frac{3}{2}\pi) \quad (3a)$$

$$b_i = r_{2i} \sin(\gamma_i + \beta_i - \frac{3}{2}\pi) \quad (3b)$$

By reminding that the distance $r_{3(i+4)}$ between the points P_{2i} and P_{1k} (see Fig. 3) can be expressed through the coordinates of the two points, measured in any Cartesian reference system, the following set of closure equations can be written for the PS under study:

$$({}^i \mathbf{P}_{2i} - {}^i \mathbf{P}_{1k})^2 = r_{3(i+4)}^2, \quad i = 1, \dots, 4; \quad k = (i+1) \text{ modulo } 4 \quad (4)$$

The introduction of the explicit expressions (2) into Eq. (4) yields the following system of closure equations in explicit form:

$$(a_i c_i - b_i s_i - r_{1k} s_k)^2 + (a_i s_i + b_i c_i - r_{0i} + r_{1k} c_k)^2 - r_{3(i+4)}^2 = 0$$

$$i = 1, \dots, 4; \quad k = (i+1) \text{ modulo } 4 \quad (5)$$

Closure equations (5) constitute a system of four scalar equations in four unknowns: the four joint variables θ_i , $i=1, \dots, 4$. By expanding Eq. (5), system (5) becomes

$$g_{i0} + g_{i1} s_i + g_{i2} c_i + g_{i3} c_k + g_{i4} (s_i c_k - c_i s_k) + g_{i5} (c_i c_k + s_i s_k) = 0$$

$$i = 1, \dots, 4; \quad k = (i+1) \text{ modulo } 4 \quad (6)$$

where the constant coefficients g_{in} , $n=0, 1, \dots, 5$, have the following explicit expressions:

$$g_{i0} = r_{2i}^2 + r_{1k}^2 + r_{0i}^2 - r_{3(i+4)}^2 \quad (7a)$$

$$g_{i1} = -2r_{0i} a_i, \quad g_{i2} = -2r_{0i} b_i, \quad g_{i3} = -2r_{0i} r_{1k} \quad (7b)$$

$$g_{i4} = 2r_{1k} a_i, \quad g_{i5} = 2r_{1k} b_i \quad (7c)$$

Each equation of system (6) is linear both in c_i and s_i and in c_k and s_k .

3.2 Spherical Structure. Figure 4 shows the spherical structure with the topology of Fig. 1. With reference to Fig. 4, O is the center of the unit sphere; Q_i for $i=1, \dots, 4$ are the points that locate, on the unit sphere, the axes of the revolute pairs that join

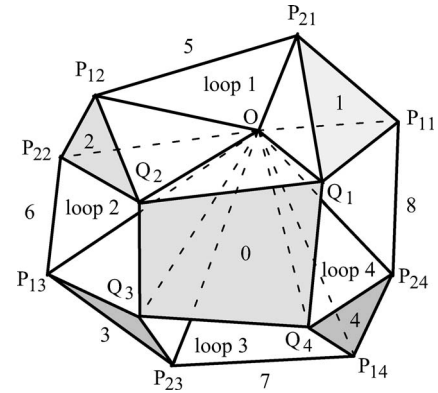


Fig. 4 Four-loop SS with the topology of Fig. 1

the quaternary link (link 0) to the i th ternary link ($i=1, \dots, 4$). P_{ji} for $j=1, 2$ and $i=1, \dots, 4$ are the points that locate, on the unit sphere, the axes of the revolute pairs that join the i th ternary link to the two adjacent binary links.

Figure 5 shows the i th loop ($i=1, \dots, 4$) of the SS and the notation that will be used to deduce its loop equation. With reference to Fig. 5, the link-index k is equal to $(i+1)$ modulo 4. ρ_{0i} is the convex central angle $\widehat{Q_i O Q_k}$. ρ_{ji} (ρ_{jk}), $j=1, 2$, is the convex central angle $\widehat{Q_i O P_{ji}}$ ($\widehat{Q_k O P_{jk}}$). And $\rho_{3(i+4)}$ is the convex central angle $\widehat{P_{2i} O P_{1k}}$. The angles β_i and γ_i (β_k and γ_k) are the dihedral angles at the edge OQ_i (OQ_k) of link i (link k) and link 0, respectively. The angle θ_i (θ_k) is the joint variable of the revolute pair located by Q_i (Q_k). Eventually, the reference system $Ox_i y_i z_i$ is a Cartesian reference system, fixed to link 0, that will be used to write the loop equation of the i th loop.

It is worth noting that the eight geometric constants of the quaternary link (i.e., γ_i and ρ_{0i} for $i=1, \dots, 4$) are related by any tern of independent scalar equations deducible from the following matrix equation (see Figs. 4 and 5):

$${}^1 \mathbf{R}_4 {}^4 \mathbf{R}_3 {}^3 \mathbf{R}_2 {}^2 \mathbf{R}_1 = \mathbf{I} \quad (8)$$

where \mathbf{I} is the 3×3 identity matrix, whereas ${}^k \mathbf{R}_i$, $k=(i+1)$ modulo 4, is the rotation matrix that transforms vector components measured in $Ox_i y_i z_i$ into vector components measured in $Ox_k y_k z_k$. ${}^k \mathbf{R}_i$ has the following explicit expression:

$${}^k \mathbf{R}_i = \mathbf{R}_x(-\rho_{0i}) \mathbf{R}_z(\pi - \gamma_k) \quad (9)$$

where the following elementary rotation matrices have been introduced:

$$\mathbf{R}_x(\alpha) = \begin{pmatrix} 1 & 0 & 0 \\ 0 & \cos \alpha & -\sin \alpha \\ 0 & \sin \alpha & \cos \alpha \end{pmatrix} \quad (10a)$$

$$\mathbf{R}_z(\alpha) = \begin{pmatrix} \cos \alpha & -\sin \alpha & 0 \\ \sin \alpha & \cos \alpha & 0 \\ 0 & 0 & 1 \end{pmatrix} \quad (10b)$$

With these notations, the position vectors of the points P_{2i} and P_{1k} , in the reference system $Ox_i y_i z_i$, have the following explicit expressions ($i=1, \dots, 4$; $k=(i+1)$ modulo 4):

⁵The measure of the convex central angle between two radius vectors gives the distance, on the unit sphere, between the two points located on the sphere by the two radius vectors.

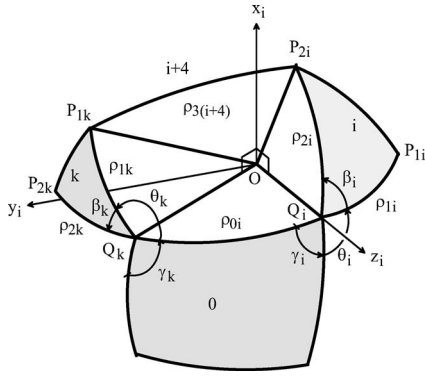


Fig. 5 i th loop of the SS: notation ($i=1, \dots, 4$; $k=(i+1)$ modulo 4)

$${}^i\mathbf{P}_{2i} = \begin{pmatrix} u_i c_i - v_i s_i \\ u_i s_i + v_i c_i \\ w_i \end{pmatrix}, \quad {}^i\mathbf{P}_{1k} = \begin{pmatrix} s_{1k} s_k \\ c_{1k} s_{0i} - s_{1k} c_{0i} c_k \\ c_{1k} c_{0i} + s_{1k} s_{0i} c_k \end{pmatrix} \quad (11)$$

where the left superscript i indicates that the vectors are measured in $Ox_i y_i z_i$. c_i (c_k) and s_i (s_k) stand for $\cos \theta_i$ ($\cos \theta_k$) and $\sin \theta_i$ ($\sin \theta_k$), respectively, whereas c_{0i} (c_{1k}) and s_{0i} (s_{1k}) stand for $\cos \rho_{0i}$ ($\cos \rho_{1k}$) and $\sin \rho_{0i}$ ($\sin \rho_{1k}$), respectively. Eventually, u_i , v_i , and w_i are geometric constants with the following explicit expressions:

$$u_i = \sin \rho_{2i} \cos\left(\gamma_i + \beta_i - \frac{3}{2}\pi\right) \quad (12a)$$

$$v_i = \sin \rho_{2i} \sin\left(\gamma_i + \beta_i - \frac{3}{2}\pi\right) \quad (12b)$$

$$w_i = \cos \rho_{2i} \quad (12c)$$

Since $\cos \rho_{3(i+4)}$ is equal to the dot product of the position vectors of the two unit-sphere points P_{2i} and P_{1k} (see Fig. 5) in any Cartesian reference system with origin at O ,⁶ the following set of closure equations can be written for the SS under study:

$${}^i\mathbf{P}_{2i}^T {}^i\mathbf{P}_{1k} = c_{3(i+4)}, \quad i = 1, \dots, 4; \quad k = (i+1) \text{ modulo } 4 \quad (13)$$

where $c_{3(i+4)}$ stands for $\cos \rho_{3(i+4)}$ and the right superscript $(\cdot)^T$ denotes the transpose of (\cdot) . The i th equation (13) analytically expresses the fact that the distance, on the unit sphere, between the two unit-sphere points P_{2i} and P_{1k} is constant; hence, it is the spherical counterpart of the i th equation (4).

The introduction of the explicit expressions (11) into Eq. (13) yields the following system of closure equations in explicit form:

$$\begin{aligned} & (u_i c_i - v_i s_i) s_{1k} s_k + (u_i s_i + v_i c_i) (c_{1k} s_{0i} - s_{1k} c_{0i} c_k) + w_i (c_{1k} c_{0i} \\ & + s_{1k} s_{0i} c_k) - c_{3(i+4)} = 0 \end{aligned} \quad (14)$$

$$i = 1, \dots, 4; \quad k = (i+1) \text{ modulo } 4$$

Closure equations (14) constitute a system of four scalar equations in four unknowns: the four joint variables θ_i , $i=1, \dots, 4$. By expanding Eq. (14), system (14) becomes

$$\begin{aligned} & h_{i0} + h_{i1} s_i + h_{i2} c_i + h_{i3} s_k + h_{i4} s_i c_k + h_{i5} c_i s_k + h_{i6} c_i c_k + h_{i7} s_i s_k = 0 \\ & i = 1, \dots, 4; \quad k = (i+1) \text{ modulo } 4 \end{aligned} \quad (15)$$

where the constant coefficients h_{in} , $n=0, 1, \dots, 7$, have the following explicit expressions:

$$h_{i0} = w_i c_{1k} c_{0i} - c_{3(i+4)}, \quad h_{i1} = u_i c_{1k} s_{0i} \quad (16a)$$

$$h_{i2} = v_i c_{1k} s_{0i}, \quad h_{i3} = w_i s_{1k} s_{0i}, \quad h_{i4} = -u_i s_{1k} c_{0i} \quad (16b)$$

$$h_{i5} = u_i s_{1k}, \quad h_{i6} = -v_i s_{1k} c_{0i}, \quad h_{i7} = -v_i s_{1k} \quad (16c)$$

Each equation of system (15) is linear both in c_i and s_i and in c_k and s_k .

4 Solution Technique

The closure-equation systems (6) and (15) can be transformed into algebraic-equation systems by using the following trigonometric identities:

$$c_i = \frac{1 - t_i^2}{1 + t_i^2}, \quad s_i = \frac{2t_i}{1 + t_i^2}, \quad i = 1, \dots, 4 \quad (17)$$

where t_i , $i=1, \dots, 4$, is equal to $\tan(\theta_i/2)$.

So doing, both systems (6) and (15) are put in the following form:

$$\sum_{n=0}^2 \sum_{m=0}^2 d_{inm} t_i^n t_k^m = 0, \quad i = 1, \dots, 4; \quad k = (i+1) \text{ modulo } 4 \quad (18)$$

where the explicit expressions of the constant coefficients d_{inm} , $n, m=0, 1, 2$, are reported in Appendixes A and B for the PS and the SS, respectively.

The first ($i=1$) and the fourth ($i=4$) equations of system (18) can be rewritten in the following form:

$$A_2 t_1^2 + A_1 t_1 + A_0 = 0 \quad (19a)$$

$$B_2 t_1^2 + B_1 t_1 + B_0 = 0 \quad (19b)$$

where $A_j = d_{1j2} t_2^2 + d_{1j1} t_2 + d_{1j0}$ and $B_j = d_{4j2} t_4^2 + d_{4j1} t_4 + d_{4j0}$ for $j=0, 1, 2$. Moreover, the second ($i=2$) and the third ($i=3$) equations of system (18) can be rewritten in the following form:

$$E_2 t_3^2 + E_1 t_3 + E_0 = 0 \quad (20a)$$

$$F_2 t_3^2 + F_1 t_3 + F_0 = 0 \quad (20b)$$

where $E_j = d_{2j2} t_2^2 + d_{2j1} t_2 + d_{2j0}$ and $F_j = d_{3j2} t_4^2 + d_{3j1} t_4 + d_{3j0}$ for $j=0, 1, 2$.

The product of Eq. (19) by t_1 yields two more equations that, when added to Eq. (19), give the following homogeneous system:

$$\mathbf{M}_1 \mathbf{f}_1 = 0 \quad (21)$$

where \mathbf{f}_1 is equal to $(t_1^3, t_1^2, t_1, 1)^T$, whereas \mathbf{M}_1 is a 4×4 matrix defined as follows:

$$\mathbf{M}_1 = \begin{pmatrix} A_2 & A_1 & A_0 & 0 \\ B_2 & B_1 & B_0 & 0 \\ 0 & A_2 & A_1 & A_0 \\ 0 & B_2 & B_1 & B_0 \end{pmatrix} \quad (22)$$

On the other hand, the product of Eq. (20) by t_3 yields two more equations that, when added to Eq. (20), give the following homogeneous system:

$$\mathbf{M}_2 \mathbf{f}_2 = 0 \quad (23)$$

where \mathbf{f}_2 is equal to $(t_3^3, t_3^2, t_3, 1)^T$, whereas \mathbf{M}_2 is a 4×4 matrix defined as follows:

$$\mathbf{M}_2 = \begin{pmatrix} E_2 & E_1 & E_0 & 0 \\ F_2 & F_1 & F_0 & 0 \\ 0 & E_2 & E_1 & E_0 \\ 0 & F_2 & F_1 & F_0 \end{pmatrix} \quad (24)$$

⁶Remind that radius vectors of the unit sphere coincide with position vectors of the unit-sphere points, located by the radius vectors, in Cartesian reference systems with origin at the unit-sphere center O .

The two homogeneous systems (21) and (23) admit nontrivial solutions for \mathbf{f}_1 and \mathbf{f}_2 , respectively, if and only if the two determinants $\det(\mathbf{M}_1)$ and $\det(\mathbf{M}_2)$ are equal to zero (i.e., their coefficient matrices are singular). Since the entries of the first and the third rows of both the matrices are quadratics in t_2 , whereas their second and fourth rows are quadratics in t_4 , the vanishing condition of $\det(\mathbf{M}_1)$ and $\det(\mathbf{M}_2)$ yields the following two algebraic equations that are quartics both in t_2 and in t_4 :

$$\sum_{n=0}^4 \sum_{m=0}^4 p_{nm} t_2^n t_4^m = 0 \quad (25a)$$

$$\sum_{n=0}^4 \sum_{m=0}^4 q_{nm} t_2^n t_4^m = 0 \quad (25b)$$

where the explicit expressions of the constant coefficients p_{nm} and q_{nm} , for $n, m=0, \dots, 4$, as functions of the constant coefficients reported in Appendixes A and B can be easily determined with the help of an algebraic manipulator. Such expressions are not reported here since they are cumbersome.

Equation (25) constitutes a nonlinear system of two equations in two unknowns: t_2 and t_4 . System (25) can be rewritten as follows:

$$\sum_{j=0}^4 L_j t_2^j = 0 \quad (26a)$$

$$\sum_{j=0}^4 N_j t_2^j = 0 \quad (26b)$$

where

$$L_j = \sum_{m=0}^4 p_{jm} t_4^m, \quad N_j = \sum_{m=0}^4 q_{jm} t_4^m, \quad j=0, \dots, 4 \quad (27)$$

The product of Eq. (26) by t_2 , t_2^2 , and t_2^3 yields six more equations that, when added to Eq. (26), give the following homogeneous system:

$$\mathbf{H}\mathbf{e} = 0 \quad (28)$$

where \mathbf{e} is equal to $(t_2^7, t_2^6, t_2^5, t_2^4, t_2^3, t_2^2, t_2, 1)^T$, whereas \mathbf{H} is an 8×8 matrix defined as follows:

$$\mathbf{H} = \begin{pmatrix} L_4 & L_3 & L_2 & L_1 & L_0 & 0 & 0 & 0 \\ N_4 & N_3 & N_2 & N_1 & N_0 & 0 & 0 & 0 \\ 0 & L_4 & L_3 & L_2 & L_1 & L_0 & 0 & 0 \\ 0 & N_4 & N_3 & N_2 & N_1 & N_0 & 0 & 0 \\ 0 & 0 & L_4 & L_3 & L_2 & L_1 & L_0 & 0 \\ 0 & 0 & N_4 & N_3 & N_2 & N_1 & N_0 & 0 \\ 0 & 0 & 0 & L_4 & L_3 & L_2 & L_1 & L_0 \\ 0 & 0 & 0 & N_4 & N_3 & N_2 & N_1 & N_0 \end{pmatrix} \quad (29)$$

The homogeneous system (28) admits nontrivial solutions for \mathbf{e} if and only if the following equation is satisfied:

$$\det(\mathbf{H}) = 0 \quad (30)$$

Since the non-null entries of matrix \mathbf{H} are univariate quartics in t_4 , and $\det(\mathbf{H})$ is a sum of terms that are products of eight entries of matrix \mathbf{H} (see Appendix C), Eq. (30) is a univariate polynomial equation in t_4 , which has at most degree 32. This result meets the upper bound to the number of complex solutions of system (18) that the authors found by calculating the optimal multihomogeneous Bézout number (see Refs. [12] and [13] for details) of system (18). Moreover, it is compatible with the number, 30, of complex solutions found in Ref. [10] for the planar case.

Once the values of t_4 that solve Eq. (30) have been computed, by back substituting them into matrix \mathbf{H} and then solving the resulting systems (28), the corresponding values of t_2 can be computed. Eventually, the computed values of the couple $\{t_2, t_4\}$ must be back substituted into Eqs. (21) and (23) to compute the corresponding values of t_1 and t_3 .

The adopted elimination procedure could have introduced extraneous solutions of type $\pm j$ with $j=\sqrt{-1}$ since the only factors, which could generate extraneous roots and have been multiplied by the original system of equations, are the factors $(1+t_i^2)(1+t_k^2)$, with $i=1, \dots, 4$ and $k=(i+1)$ modulo 4. Such factors have been used to obtain system (18) from the original ones (i.e., either Eq. (6) or Eq. (15)) passing through the trigonometric identities (17).

So far, the evaluation of the actual degree of Eq. (30) can be done either through extended numerical tests, provided that they identify at least one set of data that makes Eq. (30) a 32 deg polynomial equation, or by analytically determining the coefficients of the polynomial equation (30).

Extended numerical tests, carried out by the authors, with randomly generated data brought to find many data sets both for the planar geometry and for the spherical geometry, which make Eq. (30) a 32 deg polynomial equation. Moreover, the same numerical tests demonstrated that the elimination procedure used to obtain Eq. (30) introduces one couple of extraneous roots of type $\pm j$ in the planar case, whereas it does not introduce extraneous roots in the spherical case. These results bring to the conclusion that, in general, Eq. (30) is a 32 deg polynomial equation both for the planar geometry and for the spherical geometry, but, in the planar case, one common factor of type $(1+t_4^2)$ can always be collected and simplified. Thus, in general, the complex solutions of our problems are 30 for the planar case, which agrees with the result reported in Ref. [10], and 32 for the spherical case. Among the complex solutions of Eq. (18), only the real solutions correspond to actual assembly modes of the structure under study. For the planar case, a PS geometry with 28 assembly modes is reported in Ref. [10]. For the spherical case, the above-mentioned numerical tests brought to identify a SS geometry with 20 assembly modes. The maximum number of real solutions of Eq. (30) is still an open problem.

Regarding the analytic determination of the coefficients of the polynomial equation (30), it can be implemented with the help of an algebraic manipulator by, first, determining the explicit expression of $\det(\mathbf{H})$ as a function of the non-null entries of matrix \mathbf{H} (see Appendix C), and then elaborating the obtained expression, either as a whole or by grouping terms according to the size of the computer memory.

In the planar case, this procedure can be used to deduce the 30 deg univariate polynomial equation that contains only the complex solutions of the closure-equation system. Indeed, since, in this case, one common factor of type $(1+t_4^2)$ can be collected and simplified, Eq. (30), written in the form $\sum_{j=0}^{32} l_j t_4^j = 0$, can be put in the form $(1+t_4^2) \sum_{j=0}^{30} n_j t_4^j = 0$ by considering that the following iterative formula, which relates the n_j coefficients to the l_j coefficients, holds:

$$n_j = l_j - n_{j-2}, \quad j=0, \dots, 32 \quad (31)$$

with $n_{-2}=n_{-1}=n_{31}=n_{32}=0$.

5 Numerical Examples

Two numerical examples, one for the planar case and the other for the spherical case, are reported in this section in order to show the effectiveness of the proposed algorithm.

The algorithm has been implemented in MAPLE. The numerical computations have been executed by setting the machine precision equal to 32 decimal digits in MAPLE. All the computed solutions, when substituted into the closure equations, satisfy those equations with residuals whose absolute values range from less than

Table 1 Planar structure: solutions of the numerical example

	t_1	t_2	t_3	t_4
1	0.14540976407902879027293908	0.64496623994571841596263372	-0.33995155650823447070843769	0.0819791126793446047065806293
2	-0.077227714709025110370104775	0.76803507980135176081753200	-0.37583922874392176970779633	0.0991483691462966418039440854
3	0.31027317592256860100604449	-0.78277181236408978593774468	0.42188060295853963511347192	0.2238289048835068617548207877
4	0.45062695967325673049797405	-0.69794362132646017838199605	-0.97476498792723065506640091	0.3378809249470220693696311392
5	1.20695305556324089196099633	0.91633117401742338436255702	1.09130850106927139480659436	0.8390996311772800117631272981
6	-0.64640026596367343569314724	4.04003082965422103236594713	-2.71967984246300713821885292	1.045998408481253318241645595
7	1.66916735389394832010007919	1.14216132858181575837207037	1.37143762290017367135776656	1.050583466573429961237254444
8	13.16425818060947425215680863	4.26882828246928634814151261	-4.53789402060688689762408517	1.800982930765191163895773994
9	208.45038747133619402856213487	-2.11674168109901666421941153	-4.78562060550766382277121085	1.895978137292928399253752311
10	-26.81541066700656298137161586	-3.07760509002559592809555103	2.90357331147061231692162538	1.943292745104974910169838954
11	0.039846847673210378188216602	-1.10048431924001936505603127	0.55472513836233642331325649	-0.084308385270921315258566334
12	-0.15607071229759993578242963	-1.55698842971696026891592910	0.78641617401213709094144928	-0.167603233161461281813419201
13	0.077971500241808447357197929	0.67054918338255699388821957	0.81579796381664550087115700	-0.176970618142634298758693275
14	-0.30820112784483839462288724	-2.22324243579987649268244828	1.25223538268247267422803279	-0.302069667336494935593808144
15	-0.32498273061036110891061454	1.09252930678734718250915716	1.30746020746642945930185019	-0.316590516221194220495666284
16	0.17046575070945815221605462	0.63770346854436767382116706	-0.33797081342814258809109019	-0.363773478707546671785525565
17	-0.43210685728254645483179199	1.36268671107614166134072405	1.67488361163341613634156329	-0.407984780649443848667174677
18	0.52684373129210421002487735	-0.66739051464043879792708220	-0.93642359477505331961703787	-1.02246294842782466661923238
19	-32.55430091621347845561677664	-2.82792448537262388807377299	-253.73121491428977207738482685	-2.25282987723016144150037867
20	11.25055399577708095094706716	-1.47768067112559515995942455	-2.30168293097248032931051648	-2.42705297789839512570915480
21	10.87826714915480388273577657	3.85237293514646026565524521	-2.30523947165503596877276301	-2.43031231220896800404824993
22	10.59132861100362440506723393	3.79590172229500515671923849	-51.26410762602066041681539526	-2.43293211532249675222279903
23	-0.46091396718-0.3147647875j	0.92479484478+0.6793627405j	-0.39930489512-0.2398553778j	-0.44330155417-0.2650496400j
24	-0.46091396718+0.3147647875j	0.92479484478-0.6793627405j	-0.39930489512+0.2398553778j	-0.44330155417+0.2650496400j
25	-0.22634298550-0.3044553268j	-1.26354193430-0.9102694686j	-1.31998222381-1.436522544j	0.42996169345+0.5607327793j
26	-0.22634298550+0.3044553268j	-1.26354193430+0.9102694686j	-1.31998222381+1.436522544j	0.42996169345-0.5607327793j
27	-0.27792212930-0.2474597288j	-1.51031256094-0.9565297756j	0.65243761504+0.4943832040j	0.50950215830+0.4401832433j
28	-0.27792212930+0.2474597288j	-1.51031256094+0.9565297756j	0.65243761504-0.4943832040j	0.50950215830-0.4401832433j
29	-0.40592787199-0.3396438907j	0.84446118451+0.6023166102j	0.93036922244+0.6829091211j	0.76616003143+0.5562035841j
30	-0.40592787199+0.3396438907j	0.84446118451-0.6023166102j	0.93036922244-0.6829091211j	0.76616003143-0.5562035841j

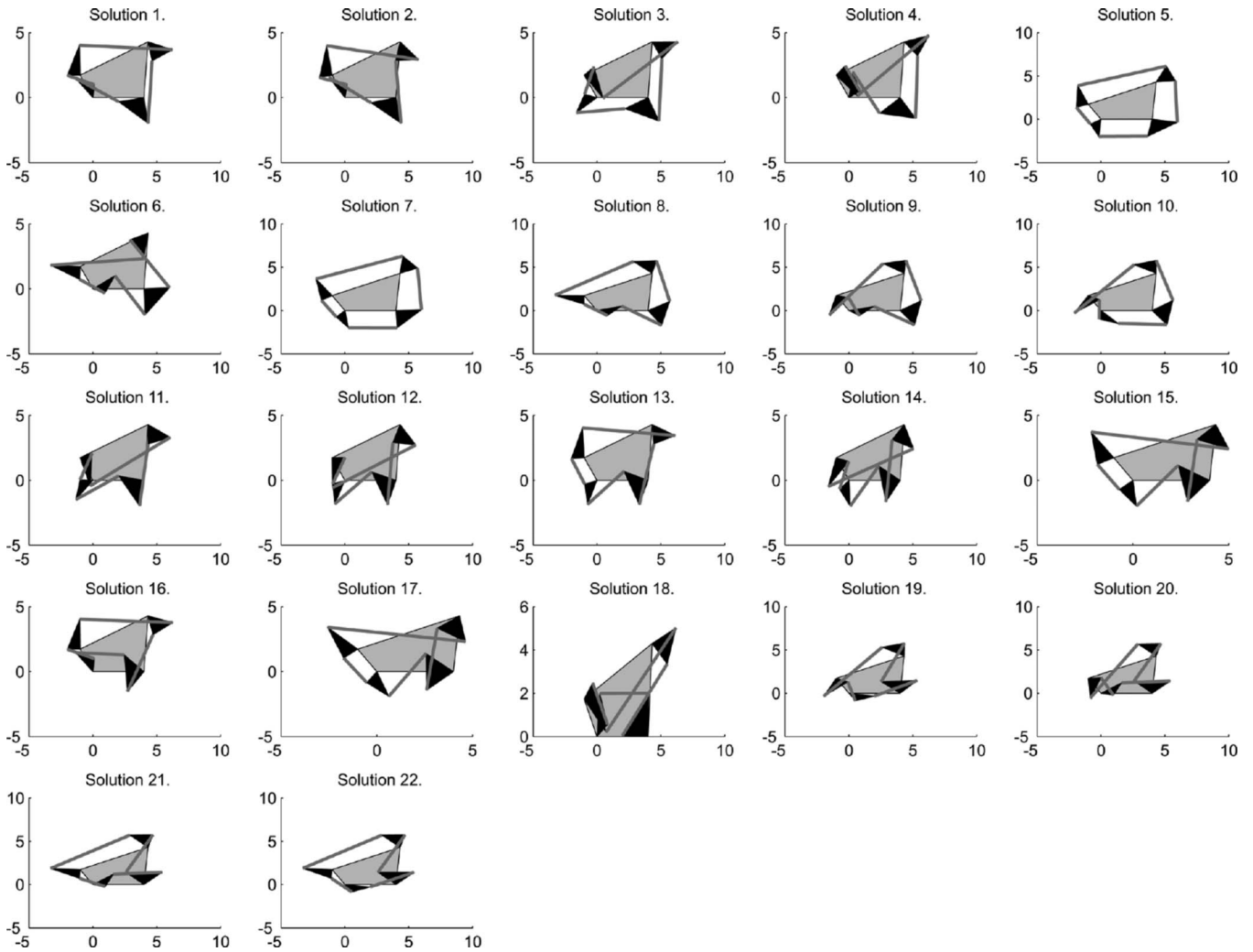


Fig. 6 Planar structure: assembly modes corresponding to the real solutions reported in Table 1

10^{-24} to 10^{-16} , which is coherent with the chosen machine precision.

5.1 Planar Structure. With reference to Fig. 3, the geometric data of the planar structure are (the angles are measured in radians; the lengths are measured in a generic unit of length) as follows:

$$\gamma_1 = \pi/3, \quad \gamma_2 = 10\pi/21, \quad \gamma_3 = 2\pi/3, \quad \gamma_4 = 11\pi/21$$

$$\beta_1 = \pi/3, \quad \beta_2 = \pi/2, \quad \beta_3 = 5\pi/18, \quad \beta_4 = \pi/2$$

$$r_{11} = 1.5, \quad r_{12} = 2.3, \quad r_{13} = 1, \quad r_{14} = 2$$

$$r_{21} = 2, \quad r_{22} = 1, \quad r_{23} = 2, \quad r_{24} = 2$$

$$r_{01} = 5.9068, \quad r_{02} = 2, \quad r_{03} = 4, \quad r_{04} = 4.3069$$

$$r_{35} = 7.2893, \quad r_{36} = 2.2485, \quad r_{37} = 3.8270, \quad r_{38} = 4.8127$$

Among these geometric data, the parameters γ_4 , r_{01} , and r_{04} have been computed by using relationships (1) together with the values of the other geometric data of the quaternary link. Moreover, once the geometries of the quaternary and the ternary links were defined, the lengths of the binary links (i.e., r_{35} , r_{36} , r_{37} , and r_{38}) have been computed through Eq. (4) after the following values of the angles θ_i , $i=1, \dots, 4$, were assigned:

$$\theta_1 = 47\pi/84, \quad \theta_2 = 17\pi/36, \quad \theta_3 = 19\pi/36, \quad \theta_4 = 4\pi/9$$

which correspond to ($t_i = \tan(\theta_i/2)$):

$$t_1 = 1.2069530555, \quad t_2 = 0.9163311740$$

$$t_3 = 1.0913085010, \quad t_4 = 0.8390996311$$

This reference assembly mode appears in Table 1 as solution 5.

All the computed solutions of system (18) for this planar geometry are reported in Table 1. Among the 30 solutions reported in Table 1, the first 22 solutions are real. Therefore the studied planar geometry admits 22 assembly modes. Such assembly modes are shown in Fig. 6.

5.2 Spherical Structure. With reference to Fig. 5, the geometric data of the spherical structure are (the angles are measured in radians) as follows:

$$\gamma_1 = \pi/6, \quad \gamma_2 = 2\pi/3, \quad \gamma_3 = 1.62440, \quad \gamma_4 = 2\pi/3$$

$$\beta_1 = \pi/4, \quad \beta_2 = \pi/4, \quad \beta_3 = \pi/6, \quad \beta_4 = \pi/4$$

$$\rho_{11} = \pi/5, \quad \rho_{12} = \pi/7, \quad \rho_{13} = \pi/5, \quad \rho_{14} = \pi/6$$

$$\rho_{21} = \pi/5, \quad \rho_{22} = \pi/7, \quad \rho_{23} = \pi/5, \quad \rho_{24} = \pi/6$$

$$\rho_{01} = 0.1855, \quad \rho_{02} = 0.1068, \quad \rho_{03} = \pi/7, \quad \rho_{04} = \pi/8$$

Table 2 Spherical structure: solutions of the numerical example

	t_1	t_2	t_3	t_4
1	0.71210618362405426284256680	-1.07497455753610126844941610	-0.44800329091214858293485363	0.08888750399467942592826241
2	-0.7755049530120851859608902	-0.74503557530432738102964660	-0.24792229123086817311120878	0.10816694054981834932287101
3	0.73108529113176738147778583	0.36104413133812455092212669	-0.23746745300156585250147610	0.10950012413553095254398550
4	-0.72549776292846969591003825	0.79320769587113511335921109	0.03630297251790967535735756	0.16000844373201842754237919
5	-0.63263922860470586533425186	-0.56652126398478751309846081	-1.44902748818508054635389670	0.27451592178874086050489859
6	1.57053701322224629303710825	-0.52991180805252246579181921	-1.37210452664695894570979698	0.68727090141199789465811756
7	2.40142765596175495890746839	0.99959051861156910688335979	1.47191403359898321689225502	0.99953905003138499326551774
8	2.94590500454578732727341691	1.14028145816754857419174148	1.68387120989711817340500497	1.14028145816754857419174148
9	-0.32795607767030026969899765	2.19663385872870672116782892	3.92448007851295936217838809	2.44302088284558462087474599
10	-0.35516231227752358582549022	-0.28916074078427804669446380	-0.94600220362422008355832889	3.26553951295171978376109941
11	-1.65975815407406043940241852	-2.56923193640685492125416214	9.79335321801512801048241709	5.03567470968899676965553945
12	-1.38917347319588278667302307	-1.84208964986328586214502214	-0.84651594808033024796061489	5.61748994274721802111609339
13	0.57581984213681238722225099	-1.30867847119402492580107470	-4.65455115661074888666990473	-0.08542804448235159783879797
14	-1.04104284673259602904066614	-1.14747508391672336044297166	-3.50406969845887886005942853	-0.10012284021138216272481265
15	-1.61463716957538962922155030	0.24467583838696498764648277	0.54597642903231132114054648	-0.36991906499149841363008628
16	0.42332462997183013284378318	0.20417982508098921066693455	0.50514822416316912555231635	-0.39495622231747702816149454
17	-2.62820087281999567358612281	-9.29741813777522859855414691	-2.57059162668172064761692181	-0.61864963851011157573145133
18	0.55460724172756564825008630	0.27238511180213352674820919	-0.30818076970875067831990899	-2.21676044670613406595744070
19	0.59483291307175496023888520	-1.26993077235092135957743913	-4.33353238096872539657203809	-2.25993333485671694287174695
20	0.90142516808676214346285897	-0.86488448942789661222868463	-0.32303829136494826043861252	-2.31799366029688446938212761
21	0.00342194452 - 1.44883692156j	-0.07299074451 - 0.36795252833j	-0.56722944684 - 0.42617220241j	-0.57746797303 - 2.18365466581j
22	0.00342194452 + 1.44883692156j	-0.07299074451 + 0.36795252833j	-0.56722944684 + 0.42617220241j	-0.57746797303 + 2.18365466581j
23	0.07455997783 - 0.12122912972j	-3.11221184246 - 3.63391279861j	-1.81717583594 - 1.05093035245j	-0.27842265152 - 1.15434019112j
24	0.07455997783 + 0.12122912972j	-3.11221184246 + 3.63391279861j	-1.81717583594 + 1.05093035245j	-0.27842265152 + 1.15434019112j
25	-0.23381078635 - 1.21762411406j	0.09063269535 - 1.17945847211j	0.04271862463 - 0.73206889984j	-0.21193805682 - 0.94629004473j
26	-0.23381078635 + 1.21762411406j	0.09063269535 + 1.17945847211j	0.04271862463 + 0.73206889984j	-0.21193805682 + 0.94629004473j
27	-0.55234273464 - 0.64624481380j	0.14522125200 - 0.66631164661j	0.32805303569 - 0.64275586423j	-0.03952558872 - 0.56289938664j
28	-0.55234273464 + 0.64624481380j	0.14522125200 + 0.66631164661j	0.32805303569 + 0.64275586423j	-0.03952558872 + 0.56289938664j
29	0.09011189540 - 1.15046250591j	0.10893422241 - 0.97670327545j	0.15179864121 - 0.99221796677j	0.07761152840 - 1.02215361384j
30	0.09011189540 + 1.15046250591j	0.10893422241 + 0.97670327545j	0.15179864121 + 0.99221796677j	0.07761152840 + 1.02215361384j
31	-0.13337931843 - 0.39981317759j	0.27358440193 - 1.79147591705j	0.32398368945 - 0.86102638956j	0.12386266728 - 0.81145941293j
32	-0.13337931843 + 0.39981317759j	0.27358440193 + 1.79147591705j	0.32398368945 + 0.86102638956j	0.12386266728 + 0.81145941293j

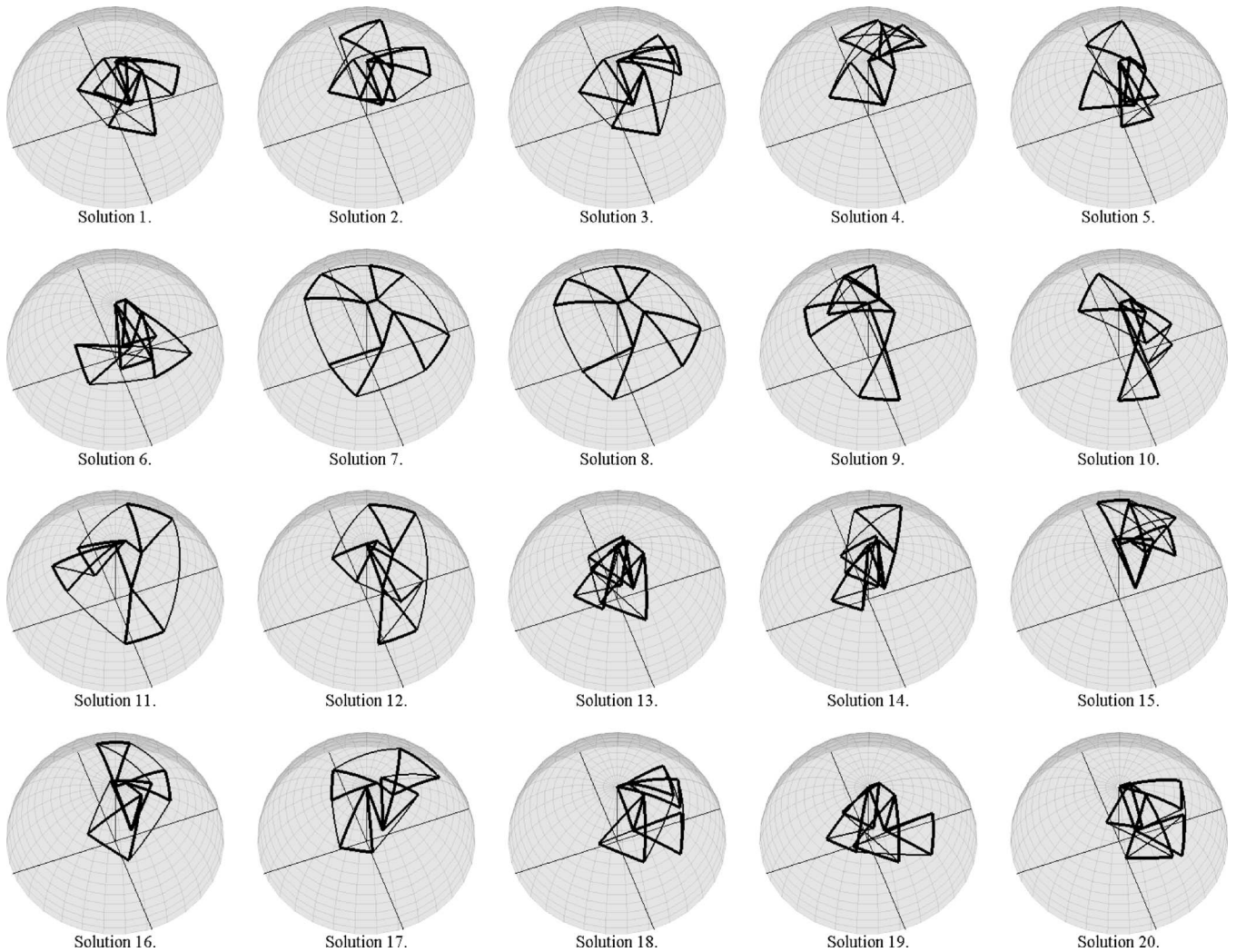


Fig. 7 Spherical structure: assembly modes corresponding to the real solutions reported in Table 2

$$\rho_{35} = 0.7099, \quad \rho_{36} = 0.4532, \quad \rho_{37} = 0.7324, \quad \rho_{38} = 0.8997$$

Among these geometric data, the angles ρ_{01} , ρ_{02} , and γ_3 have been computed by using a tern of independent scalar equations, deduced from the matrix equation (8), together with the values of the other geometric data of the quaternary link. Moreover, once the geometries of the quaternary and the ternary links were defined, the central angles of the binary links (i.e., ρ_{35} , ρ_{36} , ρ_{37} , and ρ_{38}) have been computed through Eq. (13) after the following values of the angles θ_i , $i=1, \dots, 4$, were assigned:

$$\theta_1 = 19\pi/24, \quad \theta_2 = 13\pi/24$$

$$\theta_3 = (11\pi/12) - (81/100), \quad \theta_4 = 13\pi/24$$

which correspond to ($t_i = \tan(\theta_i/2)$):

$$t_1 = 2.945905004545, \quad t_2 = 1.140281458167$$

$$t_3 = 1.683871209897, \quad t_4 = 1.140281458167$$

This reference assembly mode appears in Table 2 as solution 8.

All the computed solutions of system (18) for this spherical geometry are reported in Table 2. Among the 32 solutions reported in Table 2, the first 20 solutions are real. Therefore the studied spherical geometry admits 20 assembly modes. Such assembly modes are shown in Fig. 7.

6 Conclusions

An algorithm that determines all the assembly modes of two structures with the same topology has been presented.

The topology of the studied structures is constituted of nine links (one quaternary link, four ternary links, and four binary links) connected through 12 revolute pairs to form four closed loops.

Such structures can be thought as generated from two large families (one planar and the other spherical) of parallel manipulators by locking the actuated joints. Thus, the proposed algorithm can be used to solve the DPA of all these manipulators.

Through the proposed algorithm, it has been confirmed that the DPA of the planar manipulators, which generate structures with this topology, has 30 complex solutions. And it has been demonstrated that the DPA of their spherical counterparts has 32 complex solutions. Moreover, extended numerical tests, which used the proposed algorithm, demonstrated the robustness of the algorithm and brought to find a spherical geometry with 20 assembly modes (i.e., real solutions of the DPA). As far as the authors are aware, the analytic solution of the DPA of the spherical parallel manipulators that generate structures with this topology is new.

This work is framed into a research activity oriented to provide efficient algorithms that solve the DPA of all the planar and spherical parallel manipulators that become quadruple-loop Assur kinematic chains when their actuators are locked.

Acknowledgment

The authors wish to thank Professor Qizheng Liao and Professor Ting-Li Yang for providing important references on the subject.

This work has been partially supported by the Spanish Ministry of Education and Science, under I+D Project No. DPI2007-60858, by the 13P program with a short stay grant, and by funds of the Italian MIUR.

Appendix A

With reference to Eqs. (18) and (7), the constant coefficients d_{imm} , n , $m=0, 1, 2$, have the following explicit expressions for the planar structure (Fig. 2):

$$\begin{aligned} d_{i00} &= g_{i0} + g_{i2} + g_{i3} + g_{i5}, & d_{i10} &= 2(g_{i1} + g_{i4}) \\ d_{i01} &= -2g_{i4}, & d_{i11} &= 4g_{i5}, & d_{i20} &= g_{i0} - g_{i2} + g_{i3} - g_{i5} \\ d_{i02} &= g_{i0} + g_{i2} - g_{i3} - g_{i5}, & d_{i12} &= 2(g_{i1} - g_{i4}) \end{aligned}$$

$$d_{i21} = 2g_{i4}, \quad d_{i22} = g_{i0} - g_{i2} - g_{i3} + g_{i5}$$

Appendix B

With reference to Eqs. (18) and (16), the constant coefficients d_{imm} , n , $m=0, 1, 2$, have the following explicit expressions for the spherical structure (Fig. 4):

$$\begin{aligned} d_{i00} &= h_{i0} + h_{i2} + h_{i3} + h_{i6}, & d_{i10} &= 2(h_{i1} + h_{i4}) \\ d_{i01} &= 2h_{i5}, & d_{i11} &= 4h_{i7}, & d_{i20} &= h_{i0} - h_{i2} + h_{i3} - h_{i6} \\ d_{i02} &= h_{i0} + h_{i2} - h_{i3} - h_{i6}, & d_{i12} &= 2(h_{i1} - h_{i4}) \\ d_{i21} &= -2h_{i5}, & d_{i22} &= h_{i0} - h_{i2} - h_{i3} + h_{i6} \end{aligned}$$

Appendix C

The explicit expression of $\det(\mathbf{H})$ as a function of the non-null entries of matrix \mathbf{H} (see definition (29)) is

$$\begin{aligned} \det(\mathbf{H}) &= L_4^4 N_0^4 - L_3 L_4^3 N_0^3 N_1 + L_2 L_4^3 N_0^2 N_1^2 - L_1 L_4^3 N_0 N_1^3 + L_0 L_4^3 N_1^4 + L_3^2 L_4^2 N_0^3 N_2 - 2L_2 L_4^3 N_0^3 N_2 - L_2 L_3 L_4^2 N_0^2 N_1 N_2 + 3L_1 L_4^3 N_0^2 N_1 N_2 \\ &+ L_1 L_3 L_4^2 N_0 N_1^2 N_2 - 4L_0 L_4^3 N_0 N_1^2 N_2 - L_0 L_3 L_4^2 N_1^3 N_2 + L_2^2 L_4^2 N_0^2 N_2^2 - 2L_1 L_3 L_4^2 N_0^2 N_2^2 + 2L_0 L_4^3 N_0^2 N_2^2 - L_1 L_2 L_4^2 N_0 N_1 N_2^2 \\ &+ 3L_0 L_3 L_4^2 N_0 N_1 N_2^2 + L_0 L_2 L_4^2 N_1^2 N_2^2 + L_1^2 L_4^2 N_0 N_2^3 - 2L_0 L_2 L_4^2 N_0 N_2^3 - L_0 L_1 L_4^2 N_1 N_2^3 + L_0^2 L_4^2 N_2^4 - L_3^3 L_4 N_0^3 N_3 + 3L_2 L_3 L_4^2 N_0^3 N_3 \\ &- 3L_1 L_4^3 N_0^3 N_3 + L_2 L_3^2 L_4 N_0^2 N_1 N_3 - 2L_2^2 L_4^2 N_0^2 N_1 N_3 - L_1 L_3 L_4^2 N_0^2 N_1 N_3 + 4L_0 L_4^3 N_0^2 N_1 N_3 - L_1 L_3^2 L_4 N_0 N_1^2 N_3 + 2L_1 L_2 L_4^2 N_0 N_1^2 N_3 \\ &+ L_0 L_3 L_4^2 N_0 N_1^2 N_3 + L_0 L_3^2 L_4 N_1^3 N_3 - 2L_0 L_2 L_4^2 N_1^3 N_3 - L_2^2 L_3 L_4 N_0^2 N_2 N_3 + 2L_1 L_3^2 L_4 N_0^2 N_2 N_3 + L_1 L_2 L_4^2 N_0^2 N_2 N_3 - 5L_0 L_3 L_4^2 N_0^2 N_2 N_3 \\ &+ L_1 L_2 L_3 L_4 N_0 N_1 N_2 N_3 - 3L_0 L_3^2 L_4 N_0 N_1 N_2 N_3 - 3L_1^2 L_4^2 N_0 N_1 N_2 N_3 + 4L_0 L_2 L_4^2 N_0 N_1 N_2 N_3 - L_0 L_2 L_3 L_4 N_1^2 N_2 N_3 + 3L_0 L_1 L_4^2 N_1^2 N_2 N_3 \\ &- L_1^2 L_3 L_4 N_0 N_2^2 N_3 + 2L_0 L_2 L_3 L_4 N_0 N_2^2 N_3 + L_0 L_1 L_4^2 N_0 N_2^2 N_3 + L_0 L_1 L_3 L_4 N_1 N_2^2 N_3 - 4L_0^2 L_4^2 N_1 N_2^2 N_3 - L_0^2 L_3 L_4 N_1^2 N_3 + L_2^3 L_4 N_0^2 N_3^2 \\ &- 3L_1 L_2 L_3 L_4 N_0^2 N_3^2 + 3L_0 L_3 L_4 N_0^2 N_3^2 + 3L_1^2 L_4^2 N_0^2 N_3^2 - 3L_0 L_2 L_4^2 N_0^2 N_3^2 - L_1 L_2 L_4 N_0 N_1 N_2^3 + 2L_1^2 L_3 L_4 N_0 N_1 N_2^3 + L_0 L_2 L_3 L_4 N_0 N_1 N_2^3 \\ &- 5L_0 L_1 L_4^2 N_0 N_1 N_2^3 + L_0 L_2^2 L_4 N_1^2 N_2^3 - 2L_0 L_1 L_3 L_4 N_1^2 N_2^3 + 2L_0^2 L_4^2 N_1^2 N_2^3 + L_1^2 L_2 L_4 N_0 N_2 N_2^2 - 2L_0 L_2^2 L_4 N_0 N_2 N_2^2 - L_0 L_1 L_3 L_4 N_0 N_2 N_2^2 \\ &+ 4L_0^2 L_4^2 N_0 N_2 N_2^2 - L_0 L_1 L_2 L_4 N_1 N_2 N_2^2 + 3L_0^2 L_3 L_4 N_1 N_2 N_2^2 + L_0^2 L_2 L_4 N_1^2 N_2^2 - L_1^3 L_4 N_0 N_3^3 + 3L_0 L_1 L_2 L_4 N_0 N_3^3 - 3L_0^2 L_3 L_4 N_0 N_3^3 \\ &+ L_0 L_1 L_4^2 N_1 N_3^3 - 2L_0^2 L_2 L_4 N_1 N_3^3 - L_0^2 L_1 L_4 N_2 N_3^3 + L_0^3 L_4 N_3^4 + L_3^4 N_0^4 N_4 - 4L_2 L_3^2 L_4 N_0^3 N_4 + 2L_2^2 L_4^2 N_0^3 N_4 + 4L_1 L_3 L_4^2 N_0^3 N_4 - 4L_0 L_4^3 N_0^3 N_4 \\ &- L_2 L_3^3 N_0^2 N_1 N_4 + 3L_2^2 L_3 L_4 N_0^2 N_1 N_4 + L_1 L_3^2 L_4 N_0^2 N_1 N_4 - 5L_1 L_2 L_4^2 N_0^2 N_1 N_4 - L_0 L_3 L_4^2 N_0^2 N_1 N_4 + L_1 L_3^3 N_0 N_1^2 N_4 - 3L_1 L_2 L_3 L_4 N_0 N_1^2 N_4 \\ &- L_0 L_3^2 L_4 N_0 N_1^2 N_4 + 3L_1^2 L_4^2 N_0 N_1^2 N_4 + 2L_0 L_2 L_4^2 N_0 N_1^2 N_4 - L_0 L_3^3 N_1^3 N_4 + 3L_0 L_2 L_3 L_4 N_1^3 N_4 - 3L_0 L_1 L_4^2 N_1^3 N_4 + L_2^2 L_3^2 N_0^2 N_2 N_4 \\ &- 2L_1 L_3^3 N_0^2 N_2 N_4 - 2L_2^2 L_4 N_0^2 N_2 N_4 + 4L_1 L_2 L_3 L_4 N_0^2 N_2 N_4 + 2L_0 L_3^2 L_4 N_0^2 N_2 N_4 - 3L_1^2 L_4^2 N_0^2 N_2 N_4 + 2L_0 L_2 L_4^2 N_0^2 N_2 N_4 - L_1 L_2 L_3^2 N_0 N_1 N_2 N_4 \\ &+ 3L_0 L_3^3 N_0 N_1 N_2 N_4 + 2L_1 L_2^2 L_4 N_0 N_1 N_2 N_4 + L_1^2 L_3 L_4 N_0 N_1 N_2 N_4 - 8L_0 L_2 L_3 L_4 N_0 N_1 N_2 N_4 + 2L_0 L_1 L_4^2 N_0 N_1 N_2 N_4 + L_0 L_2 L_3^2 N_1^2 N_2 N_4 \\ &- 2L_0 L_2^2 L_4 N_1^2 N_2 N_4 - L_0 L_1 L_3 L_4 N_1^2 N_2 N_4 + 4L_0^2 L_4^2 N_1^2 N_2 N_4 + L_1^2 L_3^2 N_0 N_2^2 N_4 - 2L_0 L_2 L_3^2 N_0 N_2^2 N_4 - 2L_1^2 L_2 L_4 N_0 N_2^2 N_4 + 4L_0 L_2^2 L_4 N_0 N_2^2 N_4 \\ &- 4L_0^2 L_4^2 N_0 N_2^2 N_4 - L_0 L_1 L_3^2 N_1 N_2^2 N_4 + 2L_0 L_1 L_2 L_4 N_1 N_2^2 N_4 + L_0^2 L_3 L_4 N_1 N_2^2 N_4 + L_0^2 L_3^2 N_2^3 N_4 - 2L_0^2 L_2 L_4 N_3^3 N_4 - L_2^3 L_3 N_0^3 N_4 \\ &+ 3L_1 L_2 L_3^2 N_0^2 N_3 N_4 - 3L_0 L_3^3 N_0^2 N_3 N_4 + L_1 L_2^2 L_4 N_0^2 N_3 N_4 - 5L_1^2 L_3 L_4 N_0^2 N_3 N_4 + 2L_0 L_2 L_3 L_4 N_0^2 N_3 N_4 + 5L_0 L_1 L_4^2 N_0^2 N_3 N_4 \\ &+ L_1 L_2^2 L_3 N_0 N_1 N_3 N_4 - 2L_1^2 L_3^2 N_0 N_1 N_3 N_4 - L_0 L_2 L_3^2 N_0 N_1 N_3 N_4 - L_1^2 L_2 L_4 N_0 N_1 N_3 N_4 + 10L_0 L_1 L_3 L_4 N_0 N_1 N_3 N_4 - 8L_0^2 L_4^2 N_0 N_1 N_3 N_4 \\ &- L_0 L_2^2 L_3 N_1^2 N_3 N_4 + 2L_0 L_1 L_3^2 N_1^2 N_3 N_4 + L_0 L_1 L_2 L_4 N_1^2 N_3 N_4 - 5L_0^2 L_3 L_4 N_1^2 N_3 N_4 - L_1^2 L_2 L_3 N_0 N_2 N_3 N_4 + 2L_0 L_2^2 L_3 N_0 N_2 N_3 N_4 \\ &+ L_0 L_1 L_3^2 N_0 N_2 N_3 N_4 + 3L_1^3 L_4 N_0 N_2 N_3 N_4 - 8L_0 L_1 L_2 L_4 N_0 N_2 N_3 N_4 + 2L_0^2 L_3 L_4 N_0 N_2 N_3 N_4 + L_0 L_1 L_2 L_3 N_1 N_2 N_3 N_4 - 3L_0^2 L_3^2 N_1 N_2 N_3 N_4 \\ &- 3L_0 L_2^2 L_4 N_1 N_2 N_3 N_4 + 4L_0^2 L_2 L_4 N_1 N_2 N_3 N_4 - L_0^2 L_2 L_3 N_2^2 N_3 N_4 + 3L_0^2 L_1 L_4 N_2^2 N_3 N_4 + L_1^3 L_3 N_0 N_2^2 N_4 - 3L_0 L_1 L_2 L_3 N_0 N_2^2 N_4 \\ &+ 3L_0^2 L_3^2 N_0 N_2^2 N_4 - L_0 L_1 L_4 N_0 N_2^2 N_4 + 2L_0^2 L_2 L_4 N_0 N_2^2 N_4 - L_0 L_1^2 L_3 N_1 N_2^2 N_4 + 2L_0^2 L_2 L_3 N_1 N_2^2 N_4 + L_0^2 L_1 L_4 N_1 N_2^2 N_4 + L_0^2 L_1 L_3 N_2 N_2^2 N_4 \\ &- 4L_0^3 L_4 N_2 N_2^2 N_4 - L_0^3 L_3 N_3^3 N_4 + L_2^4 N_0^2 N_4^2 - 4L_1 L_2 L_3^2 N_0^2 N_4^2 + 2L_1^2 L_3^2 N_0^2 N_4^2 + 4L_0 L_2 L_3^2 N_0^2 N_4^2 + 4L_1^2 L_2 L_4 N_0^2 N_4^2 - 4L_0 L_2^2 L_4 N_0^2 N_4^2 \end{aligned}$$

$$\begin{aligned}
& -8L_0L_1L_3L_4N_0^2N_4^2 + 6L_0^2L_4^2N_0^2N_4^2 - L_1L_2^3N_0N_1N_4^2 + 3L_1^2L_2L_3N_0N_1N_4^2 + L_0L_2^2L_3N_0N_1N_4^2 - 5L_0L_1L_3^2N_0N_1N_4^2 - 3L_1^3L_4N_0N_1N_4^2 \\
& + 2L_0L_1L_2L_4N_0N_1N_4^2 + 5L_0^2L_3L_4N_0N_1N_4^2 + L_0L_2^3N_1^2N_4^2 - 3L_0L_1L_2L_3N_1^2N_4^2 + 3L_0^2L_3^2N_1^2N_4^2 + 3L_0L_1^2L_4N_1^2N_4^2 - 3L_0^2L_2L_4N_1^2N_4^2 \\
& + L_1^2L_2^2N_0N_2N_4^2 - 2L_0L_2^3N_0N_2N_4^2 - 2L_1^3L_3N_0N_2N_4^2 + 4L_0L_1L_2L_3N_0N_2N_4^2 - 3L_0^2L_3^2N_0N_2N_4^2 + 2L_0L_1^2L_4N_0N_2N_4^2 + 2L_0^2L_2L_4N_0N_2N_4^2 \\
& - L_0L_1L_2^2N_1N_2N_4^2 + 2L_0L_1^2L_3N_1N_2N_4^2 + L_1^2L_2L_3N_1N_2N_4^2 - 5L_0^2L_1L_4N_1N_2N_4^2 + L_0^2L_2^2N_2^2N_4^2 - 2L_0^2L_1L_3N_2^2N_4^2 + 2L_0^3L_4N_2^2N_4^2 \\
& - L_1^3L_2N_0N_3N_4^2 + 3L_0L_1L_2^2N_0N_3N_4^2 + L_0L_1^2L_3N_0N_3N_4^2 - 5L_0^2L_2L_3N_0N_3N_4^2 - L_0^2L_1L_4N_0N_3N_4^2 + L_0L_1^2L_2N_1N_3N_4^2 - 2L_0^2L_2^2N_1N_3N_4^2 \\
& - L_0^2L_1L_3N_1N_3N_4^2 + 4L_0^3L_4N_1N_3N_4^2 - L_0^2L_1L_2N_2N_3N_4^2 + 3L_0^3L_3N_2N_3N_4^2 + L_0^3L_2N_3^2N_4^2 + L_1^4N_0N_4^3 - 4L_0L_1^2L_2N_0N_4^3 + 2L_0^2L_2^2N_0N_4^3 \\
& + 4L_0^2L_1L_3N_0N_4^3 - 4L_0^3L_4N_0N_4^3 - L_0L_1^3N_1N_4^3 + 3L_0^2L_1L_2N_1N_4^3 - 3L_0^3L_3N_1N_4^3 + L_0^2L_1^2N_2N_4^3 - 2L_0^3L_2N_2N_4^3 - L_0^3L_1N_3N_4^3 + L_0^4N_4^4
\end{aligned}$$

References

- [1] Innocenti, C., 1995, "Polynomial Solution to the Position Analysis of the 7-Link Assur Kinematic Chain With One Quaternary Link," *Mech. Mach. Theory*, **30**, pp. 1295–1303.
- [2] Wampler, C. W., 2004, "Displacement Analysis of Spherical Mechanisms Having Three or Fewer Loops," *ASME J. Mech. Des.*, **126**, pp. 93–100.
- [3] Manolescu, N. I., 1973, "A Method Based on Baranov Trusses, and Using Graph Theory to Find the Set of Planar Jointed Kinematic Chains and Mechanisms," *Mech. Mach. Theory*, **8**, pp. 3–22.
- [4] Yang, T.-L., and Yao, F. H., 1988, "Topological Characteristics and Automatic Generation of Structure Analysis and Synthesis of Plane Mechanisms, Part I—Theory, Part II—Application," *Proceedings of the 1988 ASME Mechanisms Conference*, Kissimmee, FL, DE-Vol. 15-1, pp. 178–190.
- [5] Shen, H., Ting, K.-L., and Yang, T.-L., 2000, "Configuration Analysis of Complex Multiloop Linkages and Manipulators," *Mech. Mach. Theory*, **35**, pp. 353–362.
- [6] Nielsen, J., and Roth, B., 1999, "Solving the Input/Output Problem for Planar Mechanisms," *ASME J. Mech. Des.*, **121**, pp. 206–211.
- [7] Wampler, C. W., 1999, "Solving the Kinematics of Planar Mechanisms," *ASME J. Mech. Des.*, **121**, pp. 387–391.
- [8] Wampler, C. W., 2001, "Solving the Kinematics of Planar Mechanisms by Dixon Determinant and a Complex-Plane Formulation," *ASME J. Mech. Des.*, **123**, pp. 382–387.
- [9] Wang, P., Liao, Q., Zhuang, Y., and Wei, S., 2007, "A Method for Position Analysis of a Kind of Nine-Link Barranov Truss," *Mech. Mach. Theory*, **42**, pp. 1280–1288.
- [10] Han, L., Liao, Q., and Liang, C., 1999, "A Kind of Algebraic Solution for the Position Analysis of a Planar Basic Kinematic Chain," *Journal of Machine Design*, **16**(3), pp. 16–18.
- [11] Han, L., Liao, Q., and Liang, C., 2000, "Closed-Form Displacement Analysis for a Nine-Link Barranov Truss or an Eight-Link Assur Group," *Mech. Mach. Theory*, **35**, pp. 379–390.
- [12] Malajovich, G., and Meer, K., 2004, "Computing Multi-Homogeneous Bézout Numbers is Hard," Preprint, <http://www.arxiv.org/abs/cs/0405021>.
- [13] Wampler, C. W., 1992, "Bézout Number Calculations for Multi-Homogeneous Polynomial Systems," *Appl. Math. Comput.*, **51**, pp. 143–157.